arXiv:2503.15060v2 [cs.CV] 20 Mar 2025

Conjuring Positive Pairs for Efficient Unification of Representation Learning and Image Synthesis

Imanol G. Estepa*
Universitat de Barcelona, Spain
estepa.gonzalez@ub.edu

Jesús M. Rodríguez-de-Vera*
Universitat de Barcelona, Spain
j.molina.rdv@ub.edu

Ignacio Sarasúa
NVIDIA Computing Spain
isarasua@nvidia.com

Bhalaji Nagarajan
Barcelona Supercomputing Center (BSC)
bhalaji.nagarajan@bsc.es

Petia Radeva
Universitat de Barcelona, Spain
petia.ivanova@ub.edu

Abstract

While representation learning and generative modeling seek to understand visual data, unifying both domains remains unexplored. Recent Unified Self-Supervised Learning (SSL) methods have started to bridge the gap between both paradigms. However, they rely solely on semantic token reconstruction, which requires an external tokenizer during training — introducing a significant overhead. In this work, we introduce Sorcen[1]*, a novel unified SSL framework, incorporating a synergic Contrastive-Reconstruction objective. Our Contrastive objective, "Echo Contrast", leverages the generative capabilities of Sorcen, eliminating the need for additional image crops or augmentations during training. Sorcen "generates" an echo sample in the semantic token space, forming the contrastive positive pair. Sorcen operates exclusively on precomputed tokens, eliminating the need for an online token transformation during training, thereby significantly reducing computational overhead. Extensive experiments on ImageNet-1k demonstrate that Sorcen outperforms the previous Unified SSL SoTA by* ***0.4%****,* ***1.48 FID****,* ***1.76%****, and* ***1.53%*** *on linear probing, unconditional image generation, few-shot learning, and transfer learning, respectively, while being* ***60.8%*** *more efficient. Additionally, Sorcen surpasses previous single-crop MIM SoTA in linear probing and achieves SoTA performance in unconditional image generation, highlighting significant improvements and breakthroughs in Unified SSL models.*

1. Introduction

Self-Supervised Learning (SSL) and Image Synthesis are two prominent areas in Computer Vision [16, 31, 46, 56].

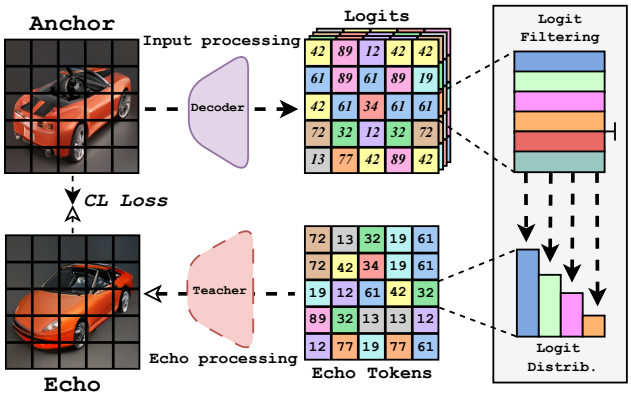


Figure 1. **Simplified Echo Contrast.** For a given anchor input, Sorcen's decoder outputs a set of logits, that are filtered to create a logit distribution, from which diverse Echo tokens are sampled. These tokens are processed by a Teacher encoder before contrasting them against the anchor. Echo contrast enables single input contrastive learning, removing the need of pixel augmentations.

While both aim to understand and represent visual data, they operate in fundamentally different ways and remain disconnected from each other [32]. SSL methods use pretext tasks such as Contrastive Representation learning [6, 10, 11, 58] and Masked Image Modeling [28, 45, 60, 65] to train general models capable of performing on multiple domains and discriminative downstream tasks. Image synthesis methods [50, 57], on the other hand, excel in learning distributions that represent the underlying visual information, capable of sampling high-fidelity images on inference when combined with an external model guidance [56, 62]. Both approaches show strong generalization within their respective domains, however, remain bounded to their specific task lines, whether discrimination or image generation.

Under representation learning, Mask Image Modeling

*Equal contribution
[1]The source is available in https://github.com/ImaGonEs/Sorcen



Figure 2. **Echo sample visualization:** Images on top correspond to decoded original token inputs that serve as an **Anchor** for the **Echo** samples (bottom). Echoes are extracted during training and decoded on a single decoding step for visualization purposes.

(MIM) showed very strong discriminative capacity, with limited image reconstruction capabilities, slightly narrowing the gap between SSL and Image synthesis [28, 60, 67]. Contrary to previous multi-crop methods [7, 13, 65] in Contrastive learning, MIM methods leverage a single image reconstruction pretext task enabling more efficient frameworks that do not depend on strong augmentations. Similarly, recent Image synthesis methods [49, 52] begin exhibiting discriminative abilities apart from their usual high-fidelity image generation. Although both families of methods support a secondary task alongside their primary function (whether discrimination or generation), their performance remains far from competitive in the other paradigm.

In both lineage, methods often require specialized setups and do not exhibit any symbiotic behavior between the primary and secondary tasks [4], i.e. the secondary task performance appears to be a consequence rather than an improvement motivating the overall performance of the model. Ideally, a "unified" model should be able to provide strong performance in both image synthesis and discrimination with an architecture that can leverage the twin strategies, improving both lines [38]. Unified SSL is driven by this need, providing models with the capacity to obtain SoTA performance in several discriminative tasks and in unconditional image generation [38]. These models exclusively rely on semantic token reconstruction pretext task, limiting their success. Recent explorations on this pretext task [38] in various setups showed that improving one of the task lines, either discriminative or generative, often decreased the other. Furthermore, creating the required semantic token space on-the-fly adds a big overhead to the already costly pretraining.

On this front, we propose a novel unified architecture, **Sorcen**, leveraging both reconstruction and contrastive pretext tasks. Our reconstruction, also based on semantic tokens, is adapted to work with precomputed tokens instead of computing them online during training, thereby completely removing a substantial overhead. Different to previous SoTA, MAGE [38], our innovative contrastive objective does not require additional multi-image setup to improve the discriminative capacity of the model, as it emerges directly from the generative ability of Sorcen. Instead of hand-made positive pairs, Sorcen generates an "Echo" sample directly from "anchors" using the reconstruction objective before contrasting both. We call this "Echo contrast" (see Figure 1). The generated Echoes provide the diversity required to perform a meaningful contrast without any supervision or common augmentations (see Figure 2).

Sorcen combines reconstruction and contrastive objectives, creating a synergy that enhances both representation learning and image generation capabilities simultaneously. We analyze the performance of Sorcen in class unconditional generation and several discriminative tasks. Compared to MAGE, Sorcen demonstrates superior performance across all tested domains and tasks, while offering improvements in efficiency in terms of memory usage and training time. Sorcen outperforms all single-crop MIM baselines and achieves top results in the unconditional image generation task. Our extensive experiments and SoTA performance introduce a novel perspective in unified SSL, while also competing with (and in some cases even surpassing) traditional SSL methods. We summarize our contributions as:

(1) We propose **Sorcen**, an innovative unified SSL method that synergistically combines contrastive and semantic reconstruction objectives, surpassing previous SoTA on both representation learning and image synthesis.

(2) We define a novel Contrastive strategy, called **Echo Contrast**, that leverages single crop reconstruction capabilities of the model to produce rich and diverse positive samples without any additional crop or pixel augmentations.

(3) Built over precomputed semantic tokens, Sorcen is the **most efficient unified SSL method**, with ≈60% reductions in training GPU hours compared to existing solutions.

(4) Our **extensive analysis** highlights the ability of Sorcen, outperforming previous unified SoTA on all tested tasks, particularly on unconditional image generation and surpassing previous single crop MIM methods on linear probing.

2. Related Works

Representation learning in Computer Vision. Traditional contrastive learning methods [10–13] have dominated unsupervised representation learning, allowing pretraining without annotations to produce models that generalize better than those trained with supervision [64]. MoCo methods [12, 13] train their models by generating image pairs from a single image using an augmentation pipeline and pulling together different representations. At the same time, the nature of popular InfoNCE loss [44] pushes away the rest of the representations, clustering the latent space without any supervised signal. While effective, these approaches suffer from the lack of sample diversity. Methods like neighbor contrast [22, 25] and synthetic positive generation [59] provide innovative strategies to increase this diversity. Given an anchor image, providing positive pairs with large intra-class variations while still belonging to the same semantic class is a hard task to do, in an uncontrolled and efficient way. Sorcen, for the first time, proposes a novel Echo-contrastive strategy that efficiently provides desired positive pairs without relying on external generative models or hand-made pixel augmentations. SimMIM [55], MAE [28] and BeiT [3] are an alternative to SSL contrastive learning approaches. Instead of relying on image pairs, MIM methods use reconstruction pretext tasks that can train models as good as the contrastive pretext task, but in a more efficient way. MAE [28], for example, uses masks up to 75% of the input images, while working with only the remaining 25%.

The increased popularity of transformers [53] and its efficiency led to rapid development of these methods. U-MAE [60] studied the dimensional collapse in MAE and proposed a novel loss to overcome it. I-JEPA [2] and XTRA [1] present architectures that further improve the efficiency of pretraining. CAE [14], CMAE [34] and iBot [64] have successfully mixed MIM with contrastive learning strategies. iBot [64] leverages multiple image crops and a self-distillation architecture to acquire visual semantics and provide SoTA results. CAE [14] and CMAE [34] require only a single sample. However, different masking strategies are applied to create positive pairs and, consequently, the same image is contrasted. In contrast, Sorcen works by providing a sample that belongs to the same semantic class, however, contains intuitive variations that make it different.

Unified SSL. While some MIM methods [28] reconstruct images, the quality of generated images differs greatly from other generation-only methods. Generative Adversarial Networks (GANs) are strong image generator with high fidelity results [8, 20, 39, 40]. Diffusion models, while more specialized in conditional generation, leverage denoising strategies to provide results on par with GANs [19, 50]. HiT [63] in GANs and DiT [49] in diffusion have further enhanced the generation quality. MaskGIT [9] used a novel generative approach capable of creating high-fidelity and high-resolution images. BigBiGAN [20], l-DAE [15] and ADDP [52] prove that generative features lead to decent image recognition results, opening an interesting line where a single SSL model could excel in both generative and image recognition tasks. MAGE [38] remains the most competitive unified SSL model. Similarly to token-based discriminative methods [37, 47], MAGE [38] leverages VQGAN [23] and proposes a semantic reconstruction objective that manages to train a model for both unconditional generation and discriminative tasks. However, VQGAN [23] introduces a dramatic overhead to the method. Its contrastive version (MAGE-C), on the other hand, sacrifices generative capabilities to improve discriminative performance. Our work, Sorcen, proposes a novel contrastive strategy that allows for the improvement of both generative and discriminative capabilities of the model. Its unique Echo-contrast strategy does not require dual-augmented images [13, 64], previously trained generative models [59] or any additional module [38] such as VQGAN. Sorcen contributes to a promising line of efficient single-image contrastive learning.

3. Our Method

Sorcen (see Figure 3) is a novel unified SSL method capable of both representation learning and unconditional image generation. Sorcen carefully combines a semantic reconstruction objective, which aims to predict the input from a masked version, and a novel contrastive learning objective, which includes *generating* a positive sample, called Echo, before contrasting it against the input. We use reconstruction capabilities of Sorcen to create Echos, making them diverse and ideal for a contrastive objective. We sample the Echos directly in the semantic token space, making it more efficient than dual-crop pixel-based methods, which additionally require an augmentation pipeline. We define this sampling and contrast strategy as Echo contrast, an innovative approach that leverages the advantages of semantic token space to produce and contrast diverse variations of the input or anchor sample. Sorcen, similar to MAGE [38], applies its learning objectives in a VQGAN-based [23] Semantic Token space rather than in a pixel space. However, Sorcen computes the semantic tokens only once, removing the overhead of using VQGAN in an online manner.

Sorcen follows the common Encoder - Decoder archi-

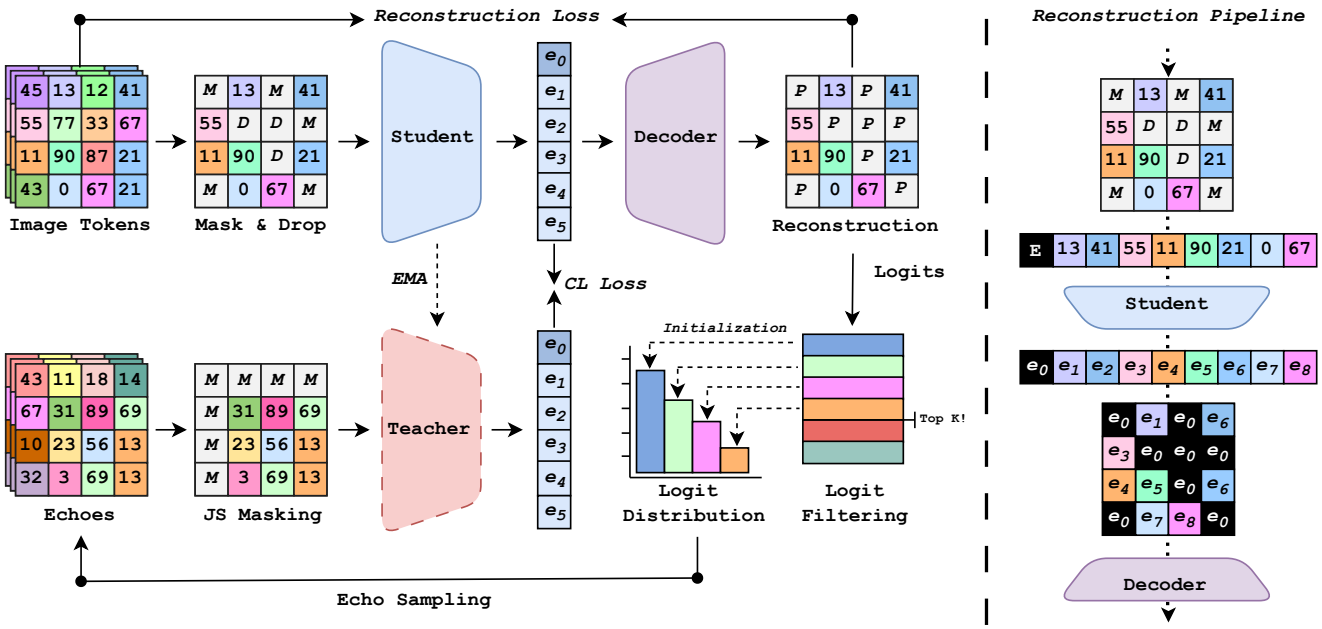


Figure 3. **Left.** Sorcen is conformed by two different objectives: (1) Semantic Reconstruction and (2) Echo Contrast. Semantic reconstruction objective masks (M) and drops (D) the input tokens before processing it by a Student encoder. The Decoder is trained to predict the original input. Using this prediction, Sorcen extracts the logits and use them to sample Echoes, which are the positive samples in Echo Contrast objective. These Echos are processed by a Teacher encoder and the loss is computed between the output of the Student and Teacher encoders. **Right.** Sorcen leverages an extra token to produce a learnable placeholder embedding for all masked and dropped tokens during the Mask&Drop phase. This ensures equal token counts for Decoder input/output, which is crucial for Semantic Reconstruction.

tecture for the reconstuction objective, defined as $\mathcal{E}$ and $\mathcal{G}$ respectively. Echo contrast, on the other hand, is performed using a Student-Teacher architecture, where the student is the encoder from the reconstruction objective. The teacher, which is a smoothed version of the student, processes the Echos before the contrastive loss, and is updated every step via Exponential Moving Average (EMA) [27, 64]. This carefully designed architecture enables a pixel-augmentation-free training that produces meaningful representations for both discriminative and generative tasks.

Input preparation. Semantic tokens capture the main concepts of images and store them in a smaller space that requires considerably less computational resources to work with. For every image $\mathcal{I}$ in the dataset $\mathcal{D}$, we precompute the sequence of semantic tokens $\mathbf{t} = (t_1, \ldots, t_{CS})$; CS is VQGAN codebook size (tokenizer). This vector $\mathbf{t}$ is made up of integers in the range $[0, v_{max}]$, where v_{max} is the tokenizer vocabulary size. This set of encoded vectors forms the Sorcen pretraining token dataset. Note that token generation phase is carried out once for each dataset and is not attached to Sorcen's pretraining phase, removing any possible overhead related to image-token transformation.

3.1. Semantic Reconstruction Objective

Our semantic reconstruction objective is divided into: Mask & Drop phase and Reconstruction objective.

Step 1: Mask & Drop. Following typical reconstruction-based methods [28, 38, 64], Sorcen randomly masks its input sequence $\mathbf{t}$, making it the groundtruth of the objective and Sorcen will be trained to reconstruct it. Sorcen follows a truncated Gaussian distribution [28], where some tokens of every input token sequence are replaced by a constant mask token, M, given a binary mask $BM = (m_i)_{i=1}^{CS}$. The Gaussian distribution is centered at 0.55 and truncated between 0.5 and 1, following MAGE [38] and MAE [28]. After masking, we further remove or drop half of the masked tokens, reducing the input size to L tokens [28, 38], thereby decreasing the computational overhead. Finally, an extra token, E, is prepended to the sequence, forming a final sequence, $\mathbf{t}'$. The extra token is prompted to learn global information about the sequence $\mathbf{t}'$, which will help in reconstruction. At the end of Mask & Drop, the token sequence, $\mathbf{t}'$ of length $L+1$ is passed through the student encoder, $\mathcal{E}$ projecting the token sequence to the unified latent space.

Step 2: Target prediction. According to the previously applied Mask & Drop binary masks, the unified latent space is adapted for the reconstruction objective. Let $\mathcal{E}(\mathbf{t}') = (e_0, e_1, \ldots, e_L)$ be the output of the encoder. We construct

a decoder input sequence $\mathbf{s} = (s_0, s_1, \ldots, s_{CS})$ by placing e_0 (the output corresponding to the prepended extra token E) in the position of every masked or dropped token. For the rest of the tokens, defined as visible tokens in reconstruction literature [28, 34, 38], the corresponding output e_i is used. This transformation process, depicted in Figure 3 (right), perfectly aligns the unified latent with the original token sequence $\mathbf{t}$ and allows proper reconstruction. Finally, the decoder $\mathcal{G}$ processes $\mathbf{s}$ to predict the original semantic token sequence $\mathbf{t}$. The reconstruction loss $\mathcal{L}_{\text{Recon}}$ is applied between the original semantic token sequence $\mathbf{t}$ and the output of $\mathcal{G}$, defined as p:

$$\mathcal{L}_{\text{Recon}} = -\mathbb{E}_{\mathbf{t}\sim\mathcal{D}}\left(\sum_{i=1}^{CS} m_i \log p(t_i|s_i)\right).$$

Following previous works [28, 34, 38], $\mathcal{L}_{\text{Recon}}$ is applied only to the masked tokens expressed by the binary mask BM.

3.2. Echo Contrast Objective

The Echo Contrast objective exploits the output of the semantic reconstruction objective to produce Echoes, the target positive samples. It is divided into 3 steps.

Step 1: Conjuring positive pairs. Sorcen uses the reconstruction capacity to generate useful positive pairs that are beneficial for contrastive learning. For every p, which contains the prediction logits generated by the decoder $\mathcal{G}$, we initialize a Categorical distribution and sample Echoes from it. We control the diversity of Echoes using only the Top-K most probable logits in the distribution. As random sampling could possibly generate an exact copy of the input as an Echo, we always skip the Top-1 logit in our Top-K filtering. Figure 2 shows some generated Echoes. The sampled Echoes retain relevant information from the anchor and provide intuitive "distortions" not achievable by common augmentation strategies. Since this process is performed in the semantic token space, the overhead is negligible.

Step 2: Jittered Spatial Masking (JSM). Inspired by pixel-based works [30, 34], we introduce spatial masking to our Echoes, increasing the diversity while providing useful information to the contrast. For each Echo, we randomly select a region of size $N \times N$ and mask the rest of the tokens using the M token. The location and size of selected region is chosen randomly during training, providing different local information each time. This spatial masking, as it maintains a region of the sequence untouched, differs from the one applied in reconstruction objective and provides different information to our contrast objective. Figure 4 visualizes this masking strategy. Once masked, the Echoes are projected to the unified latent space by our Teacher encoder.

Step 3: Pulling representations. After the JSM, the Teacher model transforms the Echo samples to obtain the corresponding hybrid latent. At this point, the processed sequence $\mathbf{t}'$ and its corresponding Echo have been projected into the unified latent space, enabling the Sorcen's contrastive objective. After applying global average pooling on both representations, InfoNCE [44] loss is applied. The process aims to pull together both anchor and Echo representations in the unified latent space. Since this loss is applied in batches, it also pushes apart the rest of the representations in the batch, dividing the space and providing better representations. Finally, an additional uniformity term is computed to the anchor representation, to increase the tokens independency and enhance the overall contrastive objective:

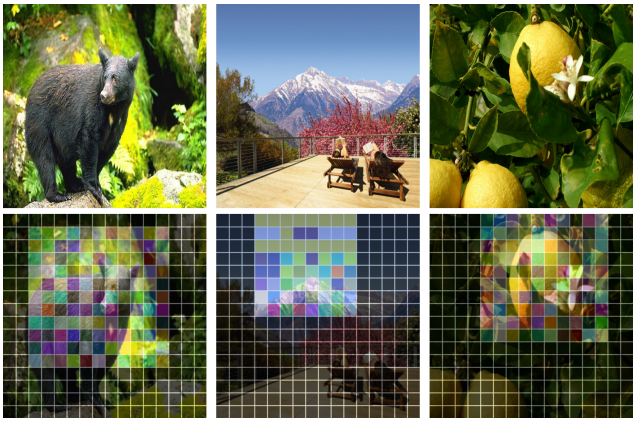


Figure 4. JSM visualization. Each cell represents a VQGAN semantic token. Gray cells are the "cropped-out" area.

$$\mathcal{L}_{\text{CL}} = -\frac{1}{B}\sum_{i=1}^{B}\log\frac{e^{z_i^T z_i'/\tau}}{\sum_{j=1}^{B} e^{z_i^T z_j'/\tau}} + 0.1\cdot\frac{1}{B}\sum_{i,j=1}^{B}\left(z_i \cdot z_j^T\right)^2$$

where $\mathbf{z}'$ and $\mathbf{z}$ represent the globally average pooled teacher and student outputs, respectively.

3.3. Sorcen Unified Objective

The final loss of Sorcen is a combination of Semantic reconstruction and Echo contrast objectives:

$$L_{Sorcen} = L_{Recon} + \lambda \cdot L_{CL}$$

where λ is the balancing hyperparameter of individual objectives. The final objective of Sorcen provides a unified representation learning objective carefully designed to improve both representation learning and image synthesis capacities of the model. Sorcen establishes as a new benchmark on unified SSL, proposing a novel symbiotic architecture and demonstrating strong SoTA performance.

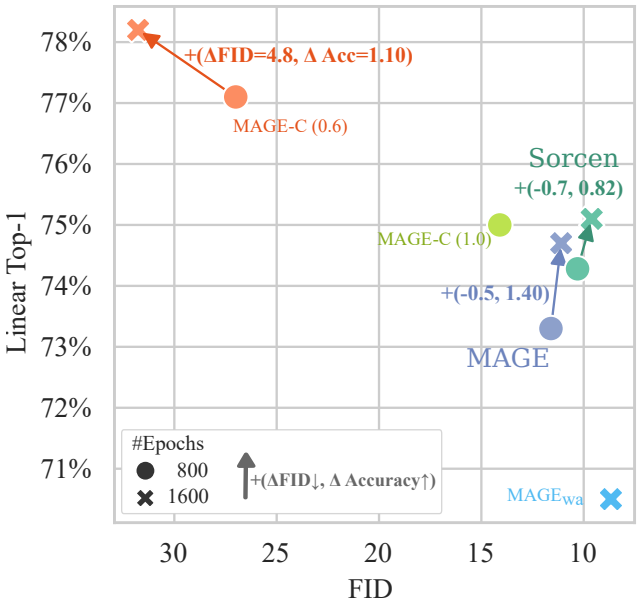


Figure 5. **Comparison of MAGE variants and Sorcen on IN1k.** Arrows illustrate the performance shift from 800 to 1600 epochs pretraining. Sorcen pushes the Pareto front for unified methods in both pre-training durations. FID (X) axis is inverted.

4. Results

We conducted extensive experiments[2] and analysis on generative and discriminative tasks, proving the capacity of Sorcen as a unified SSL framework. All experiments and pretraining (1600 epochs) are performed using ImageNet-1k [36]. For generation and discrimination evaluation, we followed MAGE [38] and MaskGIT [9], unless otherwise stated. For evaluation, only the Student encoder and the Decoder are used.

4.1. General Evaluation

Unified Evaluation. We compare the performance of Sorcen with other SoTA methods in Table 1. We divide the comparison methods in three: (1) Generative methods: Focusing on generation downstream tasks; (2) Dual image crop models: Trained with more than one view, implying multiple backward passes per training step and increased training information; (3) Single image crop models: Single image crop is used for every sample in the training set. Comparing to Generative models, Sorcen competes with recent methods such as ADDP [52], while outperforming methods such as DiT [49]. Notably, none of the generative methods manage to outperform Sorcen in linear probing. For instance, ADDP [52] obtains good results on generation, however, dramatically underperforms on linear accuracy. ViT-VQGAN [57], with its VIM-Large model (1697-M params) is a second-best competitor, with a gap of 1.9%. Qualitative image generation results are provided in Section H of Appendix. Comparing with Dual crop SSL methods, Sorcen outperforms DINO and competes with both MoCov3 [13] and iBot [64], which uses 2 augmentation views for every image in the dataset. Dual image strategy has increased the stability and performance of iBot based models by ∼2% [42] while adding significant overhead compared to single crop models. MoCov3 [13], a pure contrastive method, can't work without the augmentations. None of the models provide any generative capacities and, consequently, they fall behind Sorcen in this aspect. MAGE-C

[2] Architecture and setup details are in the Section A of the Appendix.

Methods	Model	Acc.	FID
Generative models			
DiT [49] (from [15])	DiT	62.5	30.9
l-DAE [15]	DiT-L	69.6	-
Self-Cond. GAN [39]	-	-	15.82
BigGAN$_{256}$ [5]	-	-	24.7
BigGAN+Clustering [40]	-	-	23.5
HiT [63]	HiT	-	21.64
ADM [19]	ADM	-	26.21
MaskGIT [9]	BERT	57.4	42.08
BigBiGAN [20]	RN50	56.6	21.61
ViT-VQGAN [57]	VIM-Base	65.1	-
ViT-VQGAN [57]	VIM-Large	73.2	-
IC-GAN [8]	-	-	15.6
ADDP [52]	ViT-B	11.5	8.9
Dual image crop models			
MoCov3 [13]	ViT-B	76.7	-
DINO [7]	ViT-B	72.8	-
iBot [65]	ViT-B	76.0	-
MAGE-C [38]	ViT-B	78.2	31.8
iBot$_{\text{12 crops}}$ [65]	ViT-B	79.5	-
Single image crop models			
MAE [28]	ViT-B	68.0	-
SimMIM [55]	ViT-B	57.8	-
U-MAE [60]	ViT-L	65.8	-
MI-MAE [33]	Swin-B	69.3	-
BeiT [3]	ViT-B	56.7	-
CAE [14]	ViT-B	70.4	-
CMAE [34]	ViT-B	73.9	-
XTRA [1]	ViT-B	70.2	-
I-JEPA [2]	ViT-B	72.9	-
MAGE [38]	ViT-B	74.7	11.1
Sorcen	ViT-B	**75.1**	**9.61**

Table 1. **ImageNet-1k Evaluations on linear probing (Acc.) and unconditional image generation (FID).** We divide the comparison into Generative models, which mainly focus on image generation, Dual image crop models, Representation learning methods that leverage multiple augmented views that include extra information and Single image crop models, MIM and Contrastive methods that require a single image crop. Sorcen falls under this group.

[38] on its own, sacrifices most of its generative capacities and increases its already huge VQGAN [23] overhead (2 passes are required now) to improve the linear accuracy, which "transforms" it into a discriminative only model. Sorcen clearly outperforms it on FID and competes in linear accuracy, while maintaining a good balance between discriminative and image synthesis capacities. With respect to single crop models, including vanilla MAGE [38], Sorcen outperforms previous SoTA, improving both linear accuracy and shows superior generative capabilities. While we share some similarities with CAE [14] and CMAE [34], our novel contrastive approach, based on Echo samples prove to be superior to the pixel-based contrasts. Sorcen provides a trailblazing single-crop contrastive strategy, achieving SoTA performance in unconditional image generation. Beyond outperforming single-crop methods, it also competes with multi-crop frameworks in image recognition.

MAGE vs Sorcen. Being the previous unified SSL SoTA, we compare Sorcen with all MAGE [38] versions, including MAGE-C, its contrastive variant. As shown in Figure 5, we outperform vanilla MAGE under the same setup by 0.4% on linear evaluation and 1.49 on FID. It can be noted that all MAGE versions fail to improve both metrics at the same time, being capable of incrementing only one at the cost of the other. MAGE-C, while superior in linear accuracy, is easily surpassed by Sorcen on FID metric[3]. On the other hand, MAGE$_{wa}$ falls behind Sorcen (4.6% gap in linear) while marginally outperforming by 0.94 on FID. Different MAGE versions showcase various drawbacks that hinder the original idea of unified SSL. MAGE-C, for instance, requires a dual forward-backward pass (including the VQGAN [23], see *Efficiency comparison*) to perform a contrastive objective. This however downgrades its capacity in generation. The loss of generation capacities is more pronounced when the pretraining is longer, with a significant increase in FID (Figure 5). Inversely, MAGE$_{wa}$ dramatically decreases its linear performance to boost its generation. Sorcen, with a single crop setup, outperforms vanilla MAGE [38] and competes with the "specialist" MAGE [38] variants, proving itself as a novel and efficient unified SSL SoTA. In terms of qualitative analysis, we study the benefits of the our novel Echo contrast approach (Section F of Appendix.) in improving discrimination without compromising and even improving reconstruction.

Few-shot Learning. Following [21, 38], we evaluate Sorcen's capacity to produce useful features on low data regimes. We train a single linear layer for both models and evaluate on IN1k. Compare with MAGE on 5, 10, 13 and 25 training shots of IN1k (Table 2), Sorcen consistently outperforms in all 4 setups with an average improvement of 1.76%, showing a higher representation quality.

Transfer Learning. We explore the features generated by Sorcen by evaluating them on several transfer learning setups. Following the official data splits provided by [66], a total of 7 datasets are shown in Table 3: Caltech101 [26], Flowers102 [43], OxfordPets [48], SUN397 [54], DTD [17], UCF101 [51], and EuroSAT [29]. Sorcen outperforms MAGE in 5 out of 7 seven datasets with an average improvement of 1.53%. In the remaining two datasets, it manages to obtain competitive results with less than 1% gap. Our experiments[4] prove that Sorcen, with its novel pretraining contrast, manages to learn better features that improve the generalization capacity of the backbone.

Model Robustness. Being able to produce robust representations is an important feature of any SSL algorithm. For this, we directly extract features of both Sorcen and MAGE and evaluate them against popular robustness and domain adaptation validation sets. To maintain the features of the encoder as clean as possible, we perform this evaluation using a simple k-NN over the globally pooled features of Sorcen and MAGE. As shown in Table 4, Sorcen's features prove to be more accurate w.r.t IN1k [36] and shows a higher robustness when evaluated in the rest of the validation sets. Sorcen not only outperforms MAGE but also shows a smaller drop compared to its evaluation on IN1k.

Efficiency Comparison. Previous unified methods relied heavily on VQGAN [23] inference during pretraining as

Method	Shots per ImageNet Class				
	5	10	13	25	Avg.
MAGE	48.44	57.37	59.84	63.66	57.33
Sorcen	**50.30**	**59.21**	**61.73**	**65.13**	**59.09**

Table 2. **Top-1 Accuracy for few-shot on IN1k for different number of shots per class**, as well as the average per method.

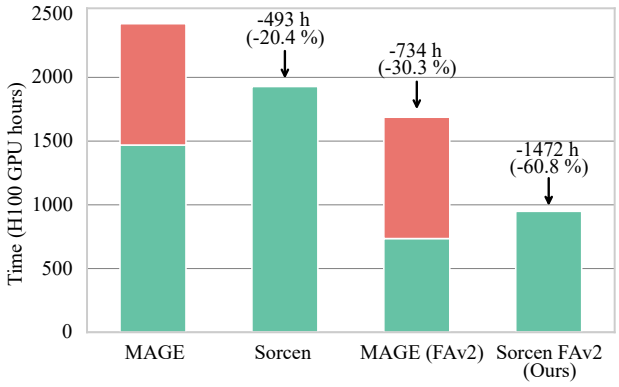


Figure 6. **Training time comparison for 1600 epochs of MAGE (left-most bar) and Sorcen (right-most bar). ■ represents the VGQAN overhead.** FAv2 stands for FlashAttention v2 [18].

[3]Table with numerical results in Section B of the Appendix.

[4]More transfer learning experiments in Section C of Appendix.

Method	Caltech	UCF101	Flowers	Pets	Sun	EuroSAT	DTD	Avg.
MAGE	88.97	59.66	**80.43**	71.38	52.36	64.44	**53.90**	67.31
Sorcen	**89.61**	**62.44**	79.50	**71.93**	**53.26**	**71.28**	53.84	**68.84**

Table 3. **Transfer learning results (top-1 accuracy) for different datasets under 16-shot settings.** Last column contains the average across datasets.

Method	IN1k	INv2	Sketch	IN-R	Avg. Drop
MAGE	60.65	45.94	14.09	22.32	33.20
Sorcen	**62.23**	**48.35**	**14.62**	**25.27**	**32.82**

Table 4. **K-NN top-1 accuracy in IN1k and 3 variants.** Average performance (↓) drop in last column.

	Echo	Echo Warm	JSM	Predictor	InfoNCE	Uniformity	L2	Top-1	FID
Sorcen$_{NoEcho}$			✓	✓	✓	✓		68.06	23.82
Sorcen$_{NoWarmup}$	✓		✓	✓	✓	✓		33.20	47.17
Sorcen$_{NoJSM}$	✓	✓		✓	✓	✓		69.30	23.05
Sorcen$_{NoPred}$	✓	✓	✓		✓	✓		69.22	**22.04**
Sorcen$_{Similarity}$	✓	✓	✓	✓		✓	✓	69.17	23.21
Sorcen$_{NoUniform}$	✓	✓	✓	✓	✓			69.12	23.66
Sorcen	✓	✓	✓	✓	✓	✓		**69.62**	22.41

Table 5. Ablation of different components of Sorcen. In each experiment (using IN200), an element of the proposal is removed during pre-training. The last two columns show results of each configuration in discriminative (few-shot top-1 accuracy) and generative (FID).

they required common pixel augmentations such as Random Resized Crop. This introduces a significant overhead in those models. In contrast, Sorcen eliminates the need for VQGAN [23] during pretraining by precomputing all tokens. In Figure 6, we compare the training times of MAGE [38] and Sorcen. Both methods are executed under same conditions, on a single H100 GPU. We also report the comparisons with FlashAttentionv2 (FAv2) [18], which is integrated into Sorcen's architecture. Sorcen is more efficient than MAGE [38], even after accounting for the additional teacher forward pass and JSM. Since our model relies solely on its transformer architecture, tools like FAv2 [18] prove more effective than in MAGE [38]. The time required by Sorcen's default setup with FAv2 [18] (∼948 H100 hours) is almost identical to the overhead introduced by VQGAN [23] in MAGE (∼951 H100 hours). Additionally, MAGE-C doubles this overhead due to the need for an extra view. Overall, Sorcen is more efficient, delivering superior results in a fraction of the training time required by MAGE [38]. Further efficiency analysis in Sec. D and E of Appendix.

4.2. Ablation Study

We highlight the importance of every design decision of Sorcen in Table 5. Due to computational limits, ablations were performed on IN200 (a 200-class subset of IN1k) for 200 epochs (1024 batch size), evaluated in a 25-shot regime.
(1) Echo Contrast. Echo pair sampling and contrast effectively boosts both discriminative and generative performance. *Sorcen*$_{NoEcho}$ shows that Echo pairs improve Top-1 by +1.5% (68.06% vs 69.62%) and reduce FID by 1.4 (23.82 vs 22.41). *Sorcen*$_{NoWarmup}$ shows the need of a warmup (10 epochs in this case) to ensure that Echo samples are relevant for contrasting. Without it, Top-1 drastically drops to 33.20% and FID raises to 47.17.
(2) JSM application. JSM further improves Echo contrast benefits. Adding JSM increases Top-1 from 69.30% ($NoJSM$) to 69.62% (full model) and reduces FID by 0.6. We expect JSM to be more impactful with longer training and larger datasets. In such scenarios, stronger decoders benefit more from JSM's ability to diversify Echo pairs capturing more nuanced semantic variations.
(3) Predictors. Different to other Teacher-student architectures, Sorcen is robust without a predictor. Removing it (*Sorcen*$_{NoPred}$) only slightly decreases Top-1, but improves FID, suggesting a trade-off: predictor favors discriminative, while its removal slightly favors generative quality.
(4) InfoNCE vs Similarity Loss. InfoNCE outperforms similarity loss, confirming our hypothesis that pushing negative samples is beneficial. While Similarity loss is competitive, InfoNCE yields a better unified feature space, though its full potential might be limited by batch size used.
(5) Uniformity Loss. Uniformity loss encourages the feature distribution to be uniformly spread across the feature space, which can be beneficial for both representation learning and generation. *Sorcen*$_{NoUniform}$ shows that removing it decreases Top-1 and increases FID, indicating a less smooth feature space and degraded generation without it.

4.3. Limitations and New Research Avenues

While Sorcen has several strengths, it also has limitations to be explored in future research. (1) Although our simple logit filtering and selection process manages to produce rich echo samples, we hypothesize that more complex approaches, such as entropy-based sampling [61], common to NLP, could further improve the echo sample quality. (2) Sorcen is limited to single echo contrast, as multiple con-

trast would require more forward passes on the Teacher model. Efficient multi-echo contrast is a potential future research. (3) Even if pre-computing the training dataset removes all training overhead, the tokenization is still required for downstream tasks as most well-established evaluation pipelines depend on pixel augmentations.

5. Conclusions

In this work, we present Sorcen, a novel unified SSL framework, significantly outperforming previous SoTA methods in both representation learning and image synthesis. Its synergic contrastive and reconstructive objectives enhances both the model's discrimination capabilities and its image generation performances. A key strength of Sorcen, the Echo Contrast, generates on-the-fly positive samples, enriching the contrastive objective with greater diversity without requiring external models or additional augmented crops. By operating on precomputed semantic tokens, Sorcen eliminates the need for token transformations during training, making it the most efficient unified SSL model within the SoTA. Extensive experiments and analysis on several discriminative tasks and unconditional image generation prove the capacity to not only excel in representation learning and image synthesis alone, but benefit from this duality. Moving forward we plan to extend Sorcen to other semantic token spaces, such as those provided by ViT-VQGAN, and to explore its potential on larger datasets.

References

[1] Elad Amrani, Leonid Karlinsky, and Alex Bronstein. Sample- and Parameter-Efficient Auto-Regressive Image Models, 2024. arXiv:2411.15648 [cs]. 3, 6

[2] Mahmoud Assran, Quentin Duval, Ishan Misra, Piotr Bojanowski, Pascal Vincent, Michael Rabbat, Yann LeCun, and Nicolas Ballas. Self-Supervised Learning From Images With a Joint-Embedding Predictive Architecture. pages 15619–15629, 2023. 3, 6

[3] Hangbo Bao, Li Dong, Songhao Piao, and Furu Wei. BEiT: BERT Pre-Training of Image Transformers. 2021. 3, 6

[4] Emily M. Bender, Timnit Gebru, Angelina McMillan-Major, and Shmargaret Shmitchell. On the Dangers of Stochastic Parrots: Can Language Models Be Too Big? . In *Proceedings of the 2021 ACM Conference on Fairness, Accountability, and Transparency*, pages 610–623, New York, NY, USA, 2021. Association for Computing Machinery. 2

[5] Andrew Brock, Jeff Donahue, and Karen Simonyan. Large Scale GAN Training for High Fidelity Natural Image Synthesis. 2018. 6

[6] Mathilde Caron, Piotr Bojanowski, Armand Joulin, and Matthijs Douze. Deep Clustering for Unsupervised Learning of Visual Features. pages 132–149, 2018. 1

[7] Mathilde Caron, Hugo Touvron, Ishan Misra, Hervé Jégou, Julien Mairal, Piotr Bojanowski, and Armand Joulin. Emerging Properties in Self-Supervised Vision Transformers. pages 9650–9660, 2021. 2, 6

[8] Arantxa Casanova, Marlene Careil, Jakob Verbeek, Michal Drozdzal, and Adriana Romero Soriano. Instance-Conditioned GAN. In *Advances in Neural Information Processing Systems*, pages 27517–27529. Curran Associates, Inc., 2021. 3, 6

[9] Huiwen Chang, Han Zhang, Lu Jiang, Ce Liu, and William T. Freeman. MaskGIT: Masked Generative Image Transformer. pages 11315–11325, 2022. 3, 6

[10] Ting Chen, Simon Kornblith, Mohammad Norouzi, and Geoffrey Hinton. A Simple Framework for Contrastive Learning of Visual Representations. In *Proceedings of the 37th International Conference on Machine Learning*, pages 1597–1607. PMLR, 2020. ISSN: 2640-3498. 1, 3

[11] Xinlei Chen and Kaiming He. Exploring Simple Siamese Representation Learning. In *2021 IEEE/CVF Conference on Computer Vision and Pattern Recognition (CVPR)*, pages 15745–15753, Nashville, TN, USA, 2021. IEEE. 1

[12] Xinlei Chen, Haoqi Fan, Ross Girshick, and Kaiming He. Improved Baselines with Momentum Contrastive Learning, 2020. arXiv:2003.04297 [cs]. 3

[13] Xinlei Chen, Saining Xie, and Kaiming He. An Empirical Study of Training Self-Supervised Vision Transformers. pages 9640–9649, 2021. 2, 3, 6

[14] Xiaokang Chen, Mingyu Ding, Xiaodi Wang, Ying Xin, Shentong Mo, Yunhao Wang, Shumin Han, Ping Luo, Gang Zeng, and Jingdong Wang. Context Autoencoder for Self-supervised Representation Learning. *International Journal of Computer Vision*, 132(1):208–223, 2024. 3, 6, 7

[15] Xinlei Chen, Zhuang Liu, Saining Xie, and Kaiming He. Deconstructing Denoising Diffusion Models for Self-Supervised Learning, 2024. arXiv:2401.14404 [cs]. 3, 6

[16] Zhihua Chen, Bo Hu, Zhongsheng Chen, and Jiarui Zhang. Progress and Thinking on Self-Supervised Learning Methods in Computer Vision: A Review. *IEEE Sensors Journal*, 24(19):29524–29544, 2024. Conference Name: IEEE Sensors Journal. 1

[17] Mircea Cimpoi, Subhransu Maji, Iasonas Kokkinos, Sammy Mohamed, and Andrea Vedaldi. Describing textures in the wild. In *Proceedings of the IEEE conference on computer vision and pattern recognition*, pages 3606–3613, 2014. 7

[18] Tri Dao. FlashAttention-2: Faster Attention with Better Parallelism and Work Partitioning. 2023. 7, 8

[19] Prafulla Dhariwal and Alex Nichol. Diffusion models beat GANs on image synthesis. In *Proceedings of the 35th International Conference on Neural Information Processing Systems*, pages 8780–8794, Red Hook, NY, USA, 2021. Curran Associates Inc. 3, 6

[20] Jeff Donahue and Karen Simonyan. Large Scale Adversarial Representation Learning. In *Advances in Neural Information Processing Systems*. Curran Associates, Inc., 2019. 3, 6

[21] Alexey Dosovitskiy, Lucas Beyer, Alexander Kolesnikov, Dirk Weissenborn, Xiaohua Zhai, Thomas Unterthiner, Mostafa Dehghani, Matthias Minderer, Georg Heigold, Sylvain Gelly, Jakob Uszkoreit, and Neil Houlsby. An Image is Worth 16x16 Words: Transformers for Image Recognition at Scale, 2021. arXiv:2010.11929 [cs]. 7

[22] Debidatta Dwibedi, Yusuf Aytar, Jonathan Tompson, Pierre Sermanet, and Andrew Zisserman. With a Little Help From My Friends: Nearest-Neighbor Contrastive Learning of Visual Representations. pages 9588–9597, 2021. 3

[23] Patrick Esser, Robin Rombach, and Bjorn Ommer. Taming Transformers for High-Resolution Image Synthesis. pages 12873–12883, 2021. 3, 7, 8, 2

[24] Imanol G Estepa, Jesús Rodríguez-de Vera, Bhalaji Nagarajan, and Petia Radeva. Good fences make good neighbours. In *Proceedings of the IEEE/CVF International Conference on Computer Vision*, pages 216–226, 2023. 2

[25] Imanol G. Estepa, Ignacio Sarasua, Bhalaji Nagarajan, and Petia Radeva. All4One: Symbiotic Neighbour Contrastive Learning via Self-Attention and Redundancy Reduction. pages 16243–16253, 2023. 3, 2

[26] Li Fei-Fei, Rob Fergus, and Pietro Perona. Learning generative visual models from few training examples: An incremental bayesian approach tested on 101 object categories. In *2004 conference on computer vision and pattern recognition workshop*, pages 178–178. IEEE, 2004. 7

[27] Jean-Bastien Grill, Florian Strub, Florent Altché, Corentin Tallec, Pierre Richemond, Elena Buchatskaya, Carl Doersch, Bernardo Avila Pires, Zhaohan Guo, Mohammad Gheshlaghi Azar, Bilal Piot, koray kavukcuoglu, Remi Munos, and Michal Valko. Bootstrap Your Own Latent - A New Approach to Self-Supervised Learning. In *Advances in Neural Information Processing Systems*, pages 21271–21284. Curran Associates, Inc., 2020. 4

[28] Kaiming He, Xinlei Chen, Saining Xie, Yanghao Li, Piotr Dollár, and Ross Girshick. Masked Autoencoders Are Scalable Vision Learners. pages 16000–16009, 2022. 1, 2, 3, 4, 5, 6

[29] Patrick Helber, Benjamin Bischke, Andreas Dengel, and Damian Borth. Eurosat: A novel dataset and deep learning benchmark for land use and land cover classification. *IEEE Journal of Selected Topics in Applied Earth Observations and Remote Sensing*, 12(7):2217–2226, 2019. 7

[30] Carlos Hinojosa, Shuming Liu, and Bernard Ghanem. ColorMAE: Exploring Data-Independent Masking Strategies in Masked AutoEncoders. In *Computer Vision – ECCV 2024*, pages 432–449, Cham, 2025. Springer Nature Switzerland. 5

[31] Vlad Hondru, Florinel Alin Croitoru, Shervin Minaee, Radu Tudor Ionescu, and Nicu Sebe. Masked Image Modeling: A Survey, 2025. arXiv:2408.06687 [cs]. 1

[32] Tianyang Hu, Fei Chen, Haonan Wang, Jiawei Li, Wenjia Wang, Jiacheng Sun, and Zhenguo Li. Complexity Matters: Rethinking the Latent Space for Generative Modeling, 2023. arXiv:2307.08283 [cs]. 1

[33] Tao Huang, Yanxiang Ma, Shan You, and Chang Xu. Learning Mask Invariant Mutual Information for Masked Image Modeling. 2024. 6

[34] Zhicheng Huang, Xiaojie Jin, Chengze Lu, Qibin Hou, Ming-Ming Cheng, Dongmei Fu, Xiaohui Shen, and Jiashi Feng. Contrastive Masked Autoencoders are Stronger Vision Learners. *IEEE Transactions on Pattern Analysis and Machine Intelligence*, 46(4):2506–2517, 2024. Conference Name: IEEE Transactions on Pattern Analysis and Machine Intelligence. 3, 5, 6, 7, 4

[35] Ziheng Jiang, Chiyuan Zhang, Kunal Talwar, and Michael C. Mozer. Characterizing Structural Regularities of Labeled Data in Overparameterized Models. In *Proceedings of the 38th International Conference on Machine Learning*, pages 5034–5044. PMLR, 2021. ISSN: 2640-3498. 4

[36] Alex Krizhevsky, Ilya Sutskever, and Geoffrey E Hinton. ImageNet Classification with Deep Convolutional Neural Networks. In *Advances in Neural Information Processing Systems*. Curran Associates, Inc., 2012. 6, 7

[37] Minhyun Lee, Song Park, Byeongho Heo, Dongyoon Han, and Hyunjung Shim. SeiT++: Masked Token Modeling Improves Storage-Efficient Training. In *Computer Vision – ECCV 2024*, pages 180–197, Cham, 2025. Springer Nature Switzerland. 3, 2, 4

[38] Tianhong Li, Huiwen Chang, Shlok Mishra, Han Zhang, Dina Katabi, and Dilip Krishnan. MAGE: MAsked Generative Encoder To Unify Representation Learning and Image Synthesis. pages 2142–2152, 2023. 2, 3, 4, 5, 6, 7, 8

[39] Steven Liu, Tongzhou Wang, David Bau, Jun-Yan Zhu, and Antonio Torralba. Diverse Image Generation via Self-Conditioned GANs. pages 14286–14295, 2020. 3, 6

[40] Mario Lučić, Michael Tschannen, Marvin Ritter, Xiaohua Zhai, Olivier Bachem, and Sylvain Gelly. High-Fidelity Image Generation With Fewer Labels. In *Proceedings of the 36th International Conference on Machine Learning*, pages 4183–4192. PMLR, 2019. ISSN: 2640-3498. 3, 6

[41] Leland McInnes, John Healy, and James Melville. Umap: Uniform manifold approximation and projection for dimension reduction. *arXiv preprint arXiv:1802.03426*, 2018. 2

[42] Théo Moutakanni, Maxime Oquab, Marc Szafraniec, Maria Vakalopoulou, and Piotr Bojanowski. You Don't Need Domain-Specific Data Augmentations When Scaling Self-Supervised Learning, 2024. arXiv:2406.09294 [cs]. 6

[43] Maria-Elena Nilsback and Andrew Zisserman. Automated flower classification over a large number of classes. In *2008 Sixth Indian conference on computer vision, graphics & image processing*, pages 722–729. IEEE, 2008. 7

[44] Aaron van den Oord, Yazhe Li, and Oriol Vinyals. Representation Learning with Contrastive Predictive Coding, 2019. arXiv:1807.03748 [cs, stat]. 3, 5

[45] Maxime Oquab, Timothée Darcet, Théo Moutakanni, Huy V. Vo, Marc Szafraniec, Vasil Khalidov, Pierre Fernandez, Daniel Haziza, Francisco Massa, Alaaeldin El-Nouby, Mido Assran, Nicolas Ballas, Wojciech Galuba, Russell Howes, Po-Yao Huang, Shang-Wen Li, Ishan Misra, Michael Rabbat, Vasu Sharma, Gabriel Synnaeve, Hu Xu, Herve Jegou, Julien Mairal, Patrick Labatut, Armand Joulin, and Piotr Bojanowski. DINOv2: Learning Robust Visual Features without Supervision. *Transactions on Machine Learning Research*, 2023. 1

[46] Utku Ozbulak, Hyun Jung Lee, Beril Boga, Esla Timothy Anzaku, Ho-min Park, Arnout Van Messem, Wesley De Neve, and Joris Vankerschaver. Know Your Self-supervised Learning: A Survey on Image-based Generative and Discriminative Training. *Transactions on Machine Learning Research*, 2023. 1

[47] Song Park, Sanghyuk Chun, Byeongho Heo, Wonjae Kim, and Sangdoo Yun. SeiT: Storage-Efficient Vision Training

with Tokens Using 1% of Pixel Storage. pages 17248–17259, 2023. 3, 2, 4

[48] Omkar M Parkhi, Andrea Vedaldi, Andrew Zisserman, and CV Jawahar. Cats and dogs. In *2012 IEEE conference on computer vision and pattern recognition*, pages 3498–3505. IEEE, 2012. 7

[49] William Peebles and Saining Xie. Scalable Diffusion Models with Transformers. pages 4195–4205, 2023. 2, 3, 6

[50] Robin Rombach, Andreas Blattmann, Dominik Lorenz, Patrick Esser, and Björn Ommer. High-Resolution Image Synthesis With Latent Diffusion Models. pages 10684–10695, 2022. 1, 3

[51] Khurram Soomro, Amir Roshan Zamir, and Mubarak Shah. Ucf101: A dataset of 101 human actions classes from videos in the wild. *arXiv preprint arXiv:1212.0402*, 2012. 7

[52] Changyao Tian, Chenxin Tao, Jifeng Dai, Hao Li, Ziheng Li, Lewei Lu, Xiaogang Wang, Hongsheng Li, Gao Huang, and Xizhou Zhu. ADDP: Learning General Representations for Image Recognition and Generation with Alternating Denoising Diffusion Process, 2024. arXiv:2306.05423 [cs]. 2, 3, 6

[53] Ashish Vaswani, Noam Shazeer, Niki Parmar, Jakob Uszkoreit, Llion Jones, Aidan N Gomez, Łukasz Kaiser, and Illia Polosukhin. Attention is All you Need. In *Advances in Neural Information Processing Systems*. Curran Associates, Inc., 2017. 3

[54] Jianxiong Xiao, James Hays, Krista A Ehinger, Aude Oliva, and Antonio Torralba. Sun database: Large-scale scene recognition from abbey to zoo. In *2010 IEEE computer society conference on computer vision and pattern recognition*, pages 3485–3492. IEEE, 2010. 7

[55] Zhenda Xie, Zheng Zhang, Yue Cao, Yutong Lin, Jianmin Bao, Zhuliang Yao, Qi Dai, and Han Hu. SimMIM: A Simple Framework for Masked Image Modeling. pages 9653–9663, 2022. 3, 6

[56] Ling Yang, Zhilong Zhang, Yang Song, Shenda Hong, Runsheng Xu, Yue Zhao, Wentao Zhang, Bin Cui, and Ming-Hsuan Yang. Diffusion Models: A Comprehensive Survey of Methods and Applications. *ACM Comput. Surv.*, 56(4): 105:1–105:39, 2023. 1

[57] Jiahui Yu, Xin Li, Jing Yu Koh, Han Zhang, Ruoming Pang, James Qin, Alexander Ku, Yuanzhong Xu, Jason Baldridge, and Yonghui Wu. Vector-quantized Image Modeling with Improved VQGAN. 2021. 1, 6

[58] Jure Zbontar, Li Jing, Ishan Misra, Yann LeCun, and Stephane Deny. Barlow Twins: Self-Supervised Learning via Redundancy Reduction. In *Proceedings of the 38th International Conference on Machine Learning*, pages 12310–12320. PMLR, 2021. ISSN: 2640-3498. 1

[59] Dewen Zeng, Yawen Wu, Xinrong Hu, Xiaowei Xu, and Yiyu Shi. Contrastive Learning with Synthetic Positives. In *Computer Vision – ECCV 2024*, pages 430–447, Cham, 2025. Springer Nature Switzerland. 3

[60] Qi Zhang, Yifei Wang, and Yisen Wang. How Mask Matters: Towards Theoretical Understandings of Masked Autoencoders. *Advances in Neural Information Processing Systems*, 35:27127–27139, 2022. 1, 2, 3, 6, 4

[61] Shimao Zhang, Yu Bao, and Shujian Huang. EDT: Improving Large Language Models' Generation by Entropy-based Dynamic Temperature Sampling, 2024. arXiv:2403.14541 [cs]. 8

[62] Zhanjie Zhang, Quanwei Zhang, Huaizhong Lin, Wei Xing, Juncheng Mo, Shuaicheng Huang, Jinheng Xie, Guangyuan Li, Junsheng Luan, Lei Zhao, Dalong Zhang, and Lixia Chen. Towards highly realistic artistic style transfer via stable diffusion with step-aware and layer-aware prompt. In *Proceedings of the Thirty-Third International Joint Conference on Artificial Intelligence*, pages 7814–7822, Jeju, Korea, 2024. 1

[63] Long Zhao, Zizhao Zhang, Ting Chen, Dimitris Metaxas, and Han Zhang. Improved Transformer for High-Resolution GANs. In *Advances in Neural Information Processing Systems*, pages 18367–18380. Curran Associates, Inc., 2021. 3, 6

[64] Jinghao Zhou, Chen Wei, Huiyu Wang, Wei Shen, Cihang Xie, Alan Yuille, and Tao Kong. Image BERT Pre-training with Online Tokenizer. 2021. 3, 4, 6

[65] Jinghao Zhou, Chen Wei, Huiyu Wang, Wei Shen, Cihang Xie, Alan Yuille, and Tao Kong. iBOT: Image BERT Pre-Training with Online Tokenizer, 2022. arXiv:2111.07832 [cs]. 1, 2, 6

[66] Kaiyang Zhou, Jingkang Yang, Chen Change Loy, and Ziwei Liu. Conditional prompt learning for vision-language models. In *IEEE/CVF Conference on Computer Vision and Pattern Recognition (CVPR)*, 2022. 7

[67] Yongxin Zhu, Bocheng Li, Hang Zhang, Xin Li, Linli Xu, and Lidong Bing. Stabilize the Latent Space for Image Autoregressive Modeling: A Unified Perspective, 2024. arXiv:2410.12490 [cs]. 2

Conjuring Positive Pairs for Efficient Unification of Representation Learning and Image Synthesis

Appendix

A. Implementation Details

Architecture details. Before the contrastive loss is applied in Sorcen, the output of the student branch is passed through a simple MLP projector of 2 layers and an MLP predictor of another 2 layers. The teacher branch is composed of a smoothed version of the student branch, including the encoder and the projector which are updated via EMA every training step. The teacher branch does not include any predictor. Reconstruction pretraining exclusively follows the student branch and includes an additional Decoder to perform the semantic reconstruction. For all experiments we use $\lambda = 0.1$, $K = 15$ and a projector size of 512 according to analysis provided in Section G.

Evaluation setup. We apply 20 steps to generate images for generative evaluation and all discriminative tasks are conducted by globally averaging the features generated by the student encoder. Teacher encoder, projectors and predictor are completely discarded on inference, using the Student encoder for discriminative tasks and the decoder for generative tasks, unless otherwise stated. To ensure reproducibility and provide a comprehensive understanding of our experimental setup, we detail the implementation specifics in this section. Tables 6, 7, and 8 summarize the key hyperparameter settings used for pre-training, linear probing, and few-shot learning experiments, respectively.

config	value
optimizer	AdamW
base learning rate	1.5e-4
weight decay	0.05
optimizer momentum	β_1, β_2 = 0.9, 0.95
batch size	4096
learning rate schedule	cosine decay
warmup epochs	40
echo warmup epochs	40
training epochs	1600
gradient clip	3.0
label smoothing	0.1
dropout	0.5
masking ratio min	0.5
masking ratio max	1.0
masking ratio mode	0.55
masking ratio std	0.25

Table 6. Pre-training Setting.

config	value
optimizer	LARS
base learning rate	0.1
weight decay	0
optimizer momentum	0.9
batch size	4096
learning rate schedule	cosine decay
warmup epochs	0
training epochs	90
augmentation	RandomResizedCrop

Table 7. Linear Probing Setting.

config	value
optimizer	LARS
base learning rate	1.0
weight decay	0.0
optimizer momentum	0.9
batch size	16
learning rate schedule	cosine decay
warmup epochs	0
training epochs	10
augmentation	RandomResizedCrop

Table 8. Few-shot Setting.

B. MAGE Multi-setup Comparison

Table 9 presents numerical results comparing MAGE and Sorcen, as visualized in Figure 5. As discussed, Sorcen improves upon the state-of-the-art in unified learning, surpassed only by specific MAGE versions that lack balanced performance in both discriminative and generative tasks, thus losing their unified model advantage.

C. Additional Transfer Learning Results

In Tables 10 and 11 we further show the transfer learning performance of Sorcen in 8 and 4 shot setups respectively. While reducing the shots, the same behaviour maintains. Sorcen firmly beats MAGE on average for both setups.

D. Precomputed MAGE

In Table 12 we compare Sorcen with a modified version of MAGE that does not include the VQGAN inference during training. Therefore, MAGE is not able to apply any of the augmentations that it relies on. Both approaches are trained

Method	Epochs	FID	Linear
MAGE	800	11.60	73.30
MAGE	1600	11.10	74.70
MAGE_{wa}	1600	8.67	70.50
MAGE-C (1.0)	800†	14.10	75.00
MAGE-C (0.6)	800†	27.00	77.10
MAGE-C (0.6)	1600†	31.77	78.20
Sorcen	800	10.30	74.28
Sorcen	1600	9.61	75.10

Table 9. Results on IN1k of different configurations of MAGE and Sorcen for 800 and 1600 pre-training epochs. † indicates the need for two passes of the VQGAN for each training step.

with the same precomputed IN200 dataset for 800 epochs and evaluated on IN200 validation and IN1k validation for 25-shot linear probing accuracy. As can be seen, MAGE falls further behind Sorcen as it was thought to be trained using, at least, Random Resized Crop augmentation which increases the diversity of the samples. This is also hinted in its Weak Augmentation setup (Table 9), where it suffers a drastic drop on discriminative performance. Sorcen has been carefully designed to train on precomputed tokens and its Echo contrast provides required diversity to the framework. This diversity makes it surpass MAGE on IN1k validation set, which includes 800 new classes for the models.

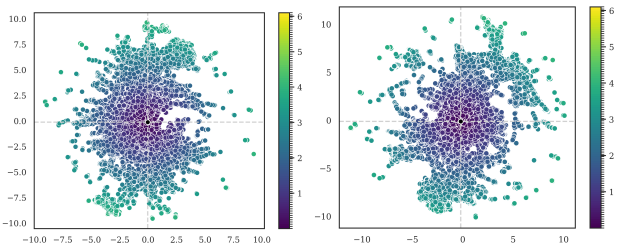
E. Disk Efficient Comparison

During training, Sorcen does not require the VQGAN tokenizer. Every image is preprocessed beforehand and we work with the processed tokens. While our main goal consists in removing the overhead provided by the VQGAN [23], we also reduce considerably the required disk space compared to the rest of the SoTA models. In Table 13, we compare Sorcen with disk-efficiency-focused models. To the best of our knowledge, Sorcen is the single disk efficient method with SoTA generation capacities. Using just the 0.29% of the original dataset size, it outperforms previous disk efficient strategies, SeiT [47] and competes with SeiT++ [37], which uses dedicated token augmentations. Our approach, using less than a third of the space used by SeiT family [37, 47], manages to produce useful features that work for both discriminative and generative tasks, something impossible for SeiT family, which exclusively work on discrimination. Even if we do not focus on disk efficient learning, Sorcen opens an interesting line where 0.39GB of preprocessed data are enough to provide SoTA discriminative and generative results. This dataset will be released upon acceptance.

F. Hybrid Space Visualization

Following other works in the literature [24, 25], we use UMAP [41] to visualize low-dimensional representations of the latent space of the model. Thanks to this visualization, we can gain insight into how elements from different semantic classes are distributed in the representation space.

Figure 7 shows the UMAP representation of the whole IN1k validation set for both MAGE and Sorcen. According to this visualization, it is easy to see that, while the MAGE space resembles a "blob", with almost no distinguishable clusters (apart from a few outliers), the space achieved by Sorcen presents easier-to-separate groups while preserving the dense nature of the MAGE space. This duality explains why Sorcen is able to excel in both discriminative and generative tasks by leveraging a common hybrid space.



(a) MAGE (b) Sorcen

Figure 7. Latent space visualization (UMAP) of MAGE and Sorcen embeddings for the IN1k validation set. Each point represents an image, colored according to its distance (in standard deviations) from the mean embedding (black dot).

To further investigate the semantic organization within the latent space, we now visualize UMAP representations, color-coded by semantic class. Figure 8 showcases these visualizations for a selection of representative classes from the IN1k training set, comparing both MAGE and Sorcen models. This class-based coloring allows us to examine the degree of separability between different semantic categories in each model's latent space, particularly for fine-grained categories.

Across the visualized classes, a consistent trend is observed: Sorcen's latent space exhibits markedly superior class separability compared to MAGE. While both models display some intra-class dispersion and inter-class mixing, this phenomenon is significantly more pronounced in MAGE. In Sorcen's representation, semantic classes are notably more distinct and less intermingled.

This enhanced class separability in Sorcen's latent space provides further insight into its hybrid capabilities. The formation of more well-defined and separated class clusters likely underpins its stronger discriminative performance. Simultaneously, the preservation of an overall dense latent space, as demonstrated previously, still accommodates generative flexibility. Consequently, these class-based UMAP

Method	Caltech	UCF101	Flowers	Pets	Sun	EuroSAT	DTD	Avg.
MAGE	83.94	46.37	**68.33**	48.79	43.38	40.01	**40.13**	52.99
Sorcen	**85.31**	**50.70**	67.37	**50.89**	**44.65**	**46.70**	39.60	**55.03**

Table 10. **Transfer learning results (top-1 accuracy) for different datasets under 8-shot settings.** Last column contains the average across datasets.

Method	Caltech	UCF101	Flowers	Pets	Sun	EuroSAT	DTD	Avg.
MAGE	**71.72**	29.71	**46.00**	24.69	31.36	18.75	19.92	34.59
Sorcen	69.20	**36.35**	43.89	**24.91**	**33.48**	**25.01**	**21.99**	**36.40**

Table 11. **Transfer learning results (top-1 accuracy) for different datasets under 4-shot settings.** Last column contains the average across datasets.

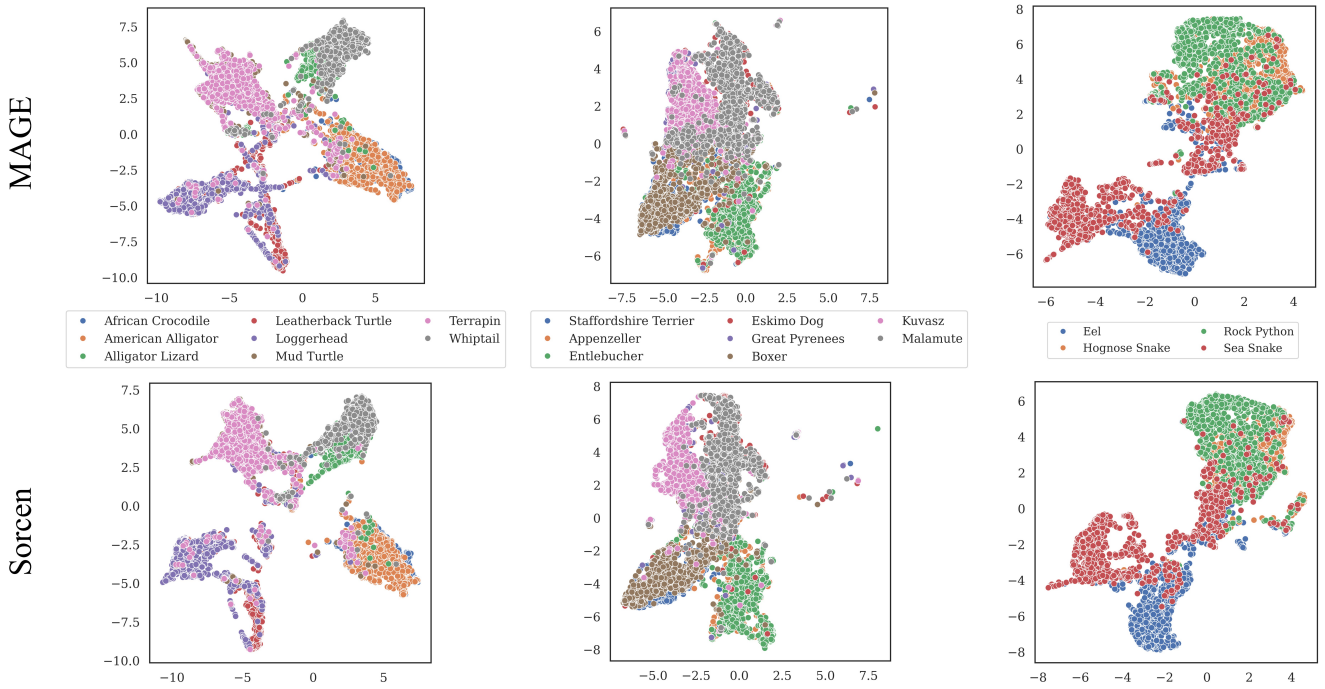


Figure 8. Class-specific UMAP visualizations of latent embeddings from MAGE (top row) and Sorcen (bottom row) for the IN1k training set. Points are colored by semantic class to illustrate class separation within each model's latent space.

Method	IN1k val †	IN200 val
MAGE$_{precomp}$	33.25	69.80
Sorcen	**36.15**	**74.10**

Table 12. **Results on precomputed token setups.** We highlight IN1k val with a † as it includes 800 new classes for the models, acting as new domain and showing the generalization capabilities of the models.

visualizations strongly suggest that Sorcen achieves a more semantically structured hybrid space. This structure effectively balances discriminative and generative representation learning, contrasting with MAGE's comparatively less organized latent space.

G. Impact of Hyperparameters

In this section, we delve into the impact of key hyperparameters on the performance of our Sorcen model. Through a series of ablation studies, we analyze the influence of the contrastive loss coefficient λ, the K parameter in top-k logit sampling, and the projector size. Due to computational constraints, we run these experiments on IN200 dataset for 200 epochs (1024 batch size) and evaluate them on few-shot regime with 25 shots per class.

Method	# of images	Storage size	Top-1	FID
MAGE [38]	1,281k	140GB (100%)	74.7	11.1
Uniform†	512k	54.6 GB (39%)	74.0	-
C-score† [35]	512k	53.3 GB (38%)	73.3	-
JPEG 5†	1,281k	11.0 GB (8%)	74.6	-
SeiT [47]	1,281k	1.4 GB (1%)	74.0	-
SeiT++ [37]	1,281k	1.4 GB (1%)	**77.8**	-
Sorcen	1,281k	**0.39 GB (0.29%)**	75.1	**9.61**

Table 13. **Storage-efficient evaluation.** Linear accuracy and FID are provided. Sorcen is the single storage-efficient method with image generation capabilities. † results reported in [47].

	0.01	0.1	1.0
Top1	66.77	69.62	47.77
FID	22.60	22.41	46.82

Table 14. Study of the impact of the value of the contrastive loss coefficient λ in accuracy (linear probing) and FID in IN200.

Contrastive loss coefficient. We ablate the contrastive loss coefficient in Table 14. Consistent with prior work [34, 38, 60], reconstruction remains the dominant loss. However, reducing it below 0.1 inhibits the advantages provided by our echoed contrast, reducing the overall performance of the system. However, our ablation in Table 14 reveals that the contrastive loss is essential. Reducing the coefficient to 0.01 leads to a decrease in Top-1 accuracy to 66.77% and a slight increase in FID to 22.60. In contrast, increasing the coefficient to 1.0 drastically degrades both metrics, with Top-1 accuracy falling to 47.77% and FID increasing significantly to 46.82. This highlights that a balanced coefficient of 0.1 effectively balances discriminative and generative performance, achieving a good trade-off in Top-1 accuracy and a low FID score.

K logit sampling. Sorcen exhibits remarkable robustness to the K parameter in top-k logit sampling ask proved in Table 15. While larger K values introduce a potential risk of sampling less accurate tokens, the skewed nature of the logits produced by the decoder mitigates negative impacts. Conversely, smaller K reduces this risk but might also limit echo sample diversity. Empirical results show negligible performance variation across K=5, 15, and 30, with Top-1 accuracy hovering around 69.6% and FID consistently low (approximately 22.4-22.8). We opted for K=15 as a balanced choice, mitigating inaccuracy risks while maintaining sufficient diversity in echo samples.

Projector size. Sorcen achieves effective contrastive learning without requiring an excessively large projector. Table 16 shows that increasing projector size beyond 512 dimensions does not yield further performance gains. In fact, expanding from 256 to 512 improves Top-1 accuracy (69.36% to 69.62%) and FID (22.74 to 22.41), indicating that 512 dimensions sufficiently capture relevant semantic information for contrast. However, further enlargement to 1024 and 2048 dimensions provides no significant advantage and even slightly degrades performance, suggesting diminishing returns and potential introduction of unnecessary model complexity beyond a projector size of 512.

	5	15	30
Top1	69.66	69.62	69,60
FID	22.69	22.41	22.77

Table 15. Study of the impact of the number of tokens, K, considered to create the echos. Results correspond to IN200 pre-training and evaluation: linear probing and FID.

	256	512	1024	2048
Top1	69.36	69.62	69.55	69.45
FID	22.74	22.41	22.52	22.19

Table 16. Impact of the size of the projector in top-1 accuracy (linear probing) and FID in IN200.

H. Qualitative Results

Thanks to the SoTA image generation achieved by Sorcen, we are able to show in this section different generative applications of this model to modify and generate high-quality images. This can be done completely from scratch (unconditioned generation) or from a given part of an image. We also exhibit randomly selected Echos from Sorcens pretraining. All the images shown in this section have been generated by Sorcen ViT-B trained for 1600 epochs on IN1k.

Echos extracted during training. In Figures 13 and 14 we display some of the Echos generated by Sorcen during training.

Unconditioned generation. Figure 9 contains 63 examples of images randomly generated by Sorcen in an unconditioned way.

Image inpainting/outpainting and reconstruction. Figures 10 to 12 contain examples of inpainting, outpainting and reconstruction applied to images from IN1k dataset. Each rows correspond to an image. For reconstruction, we use a random mask of 75% of the image. The first column is the original image, and the next columns contain pairs masked image-generation for three masks.

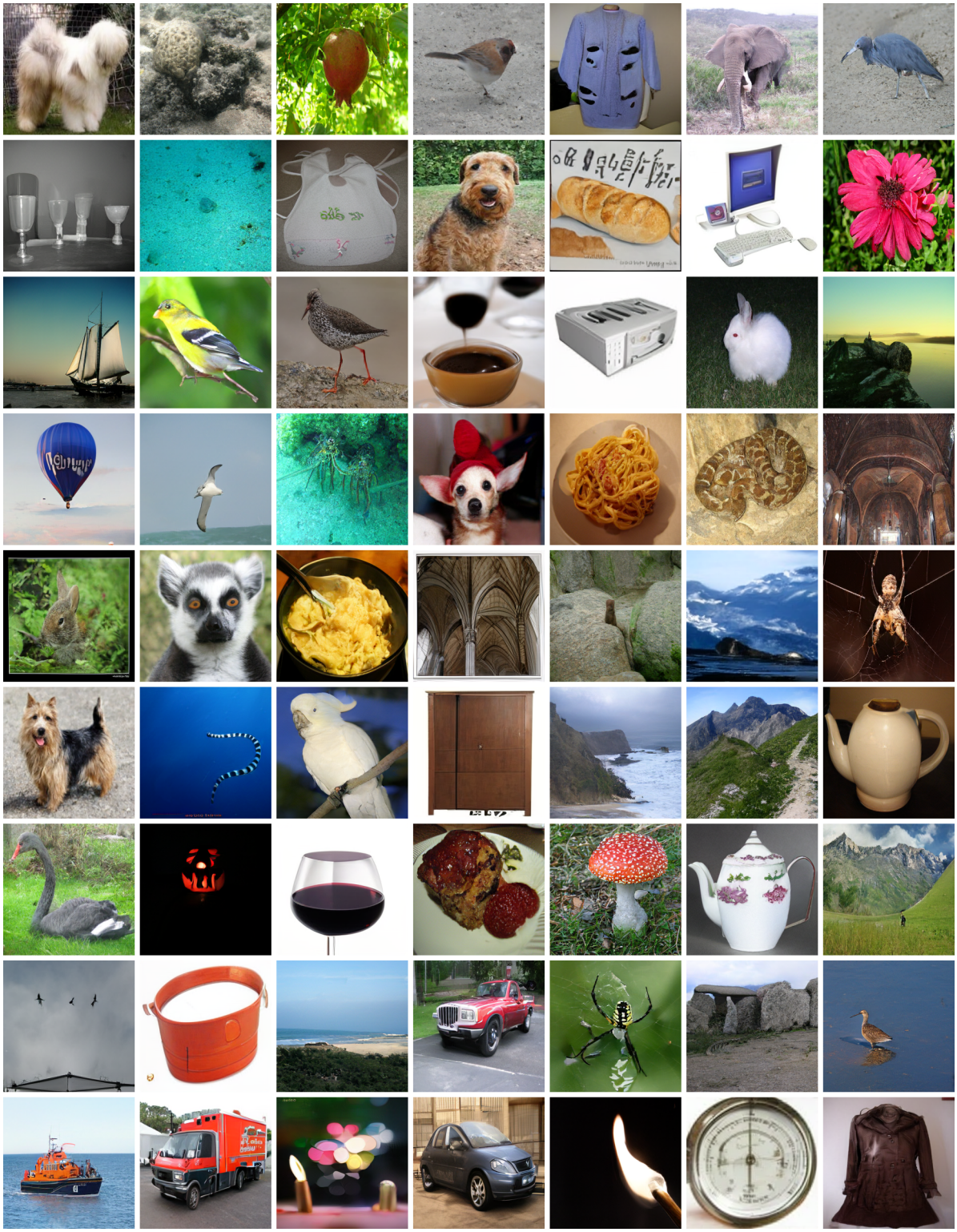


Figure 9. Images randomly generated by Sorcen in an unconditioned way using a ViT-B.

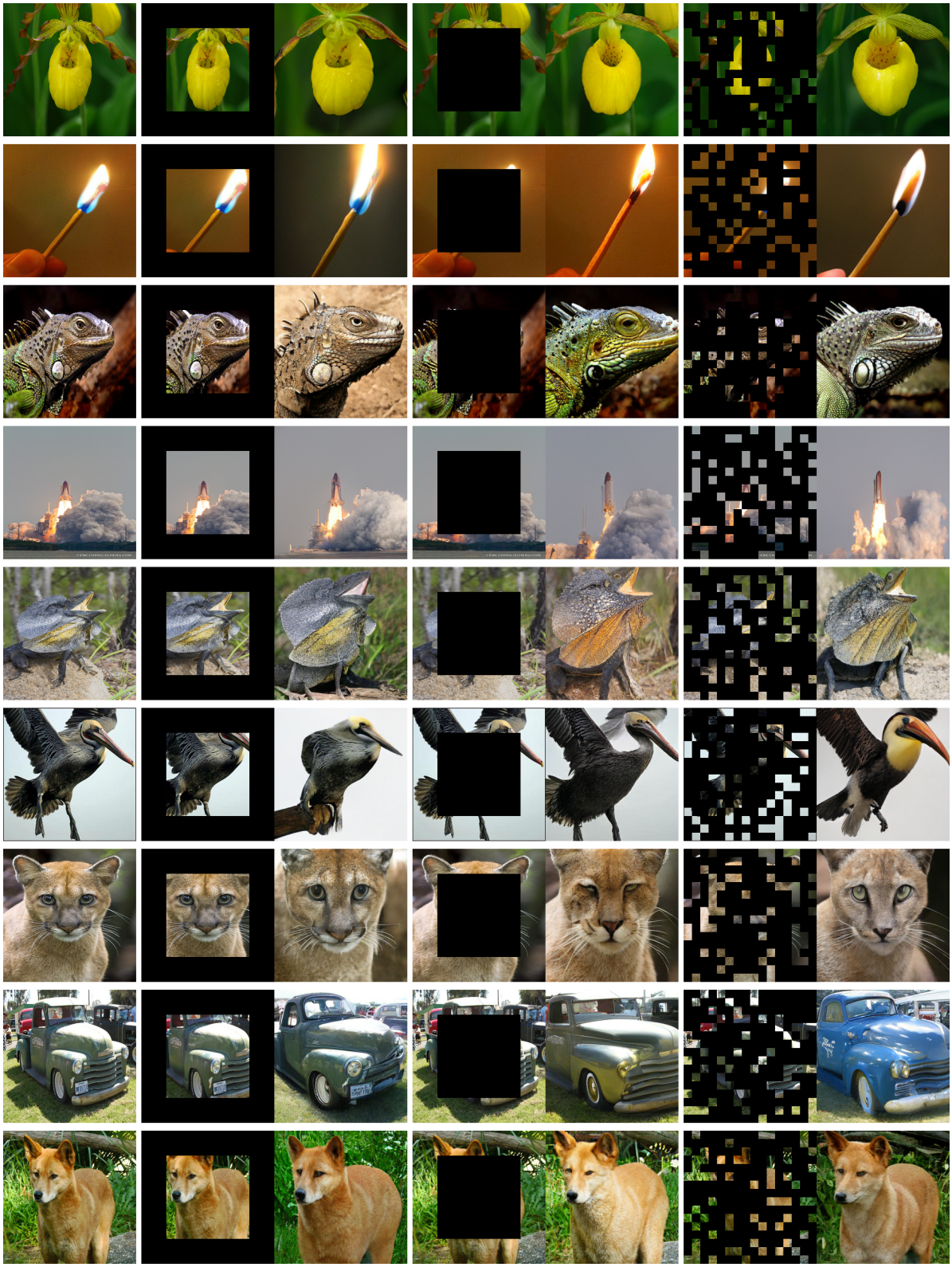


Figure 10. Examples of image inpainting, outpainting and reconstruction with Sorcen ViT-B. The first column is the original image.

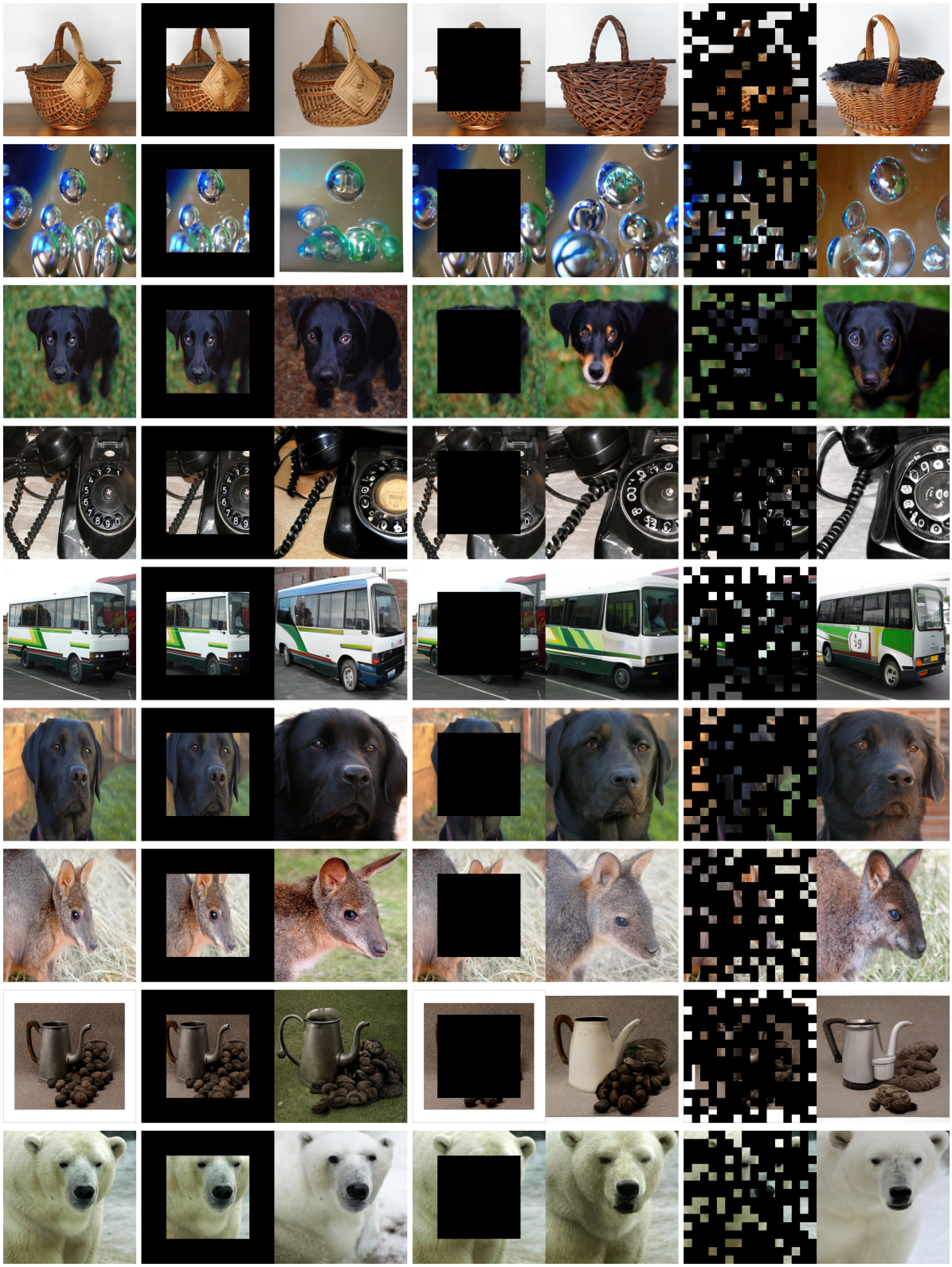


Figure 11. Examples of image inpainting, outpainting and reconstruction with Sorcen ViT-B. The first column is the original image.

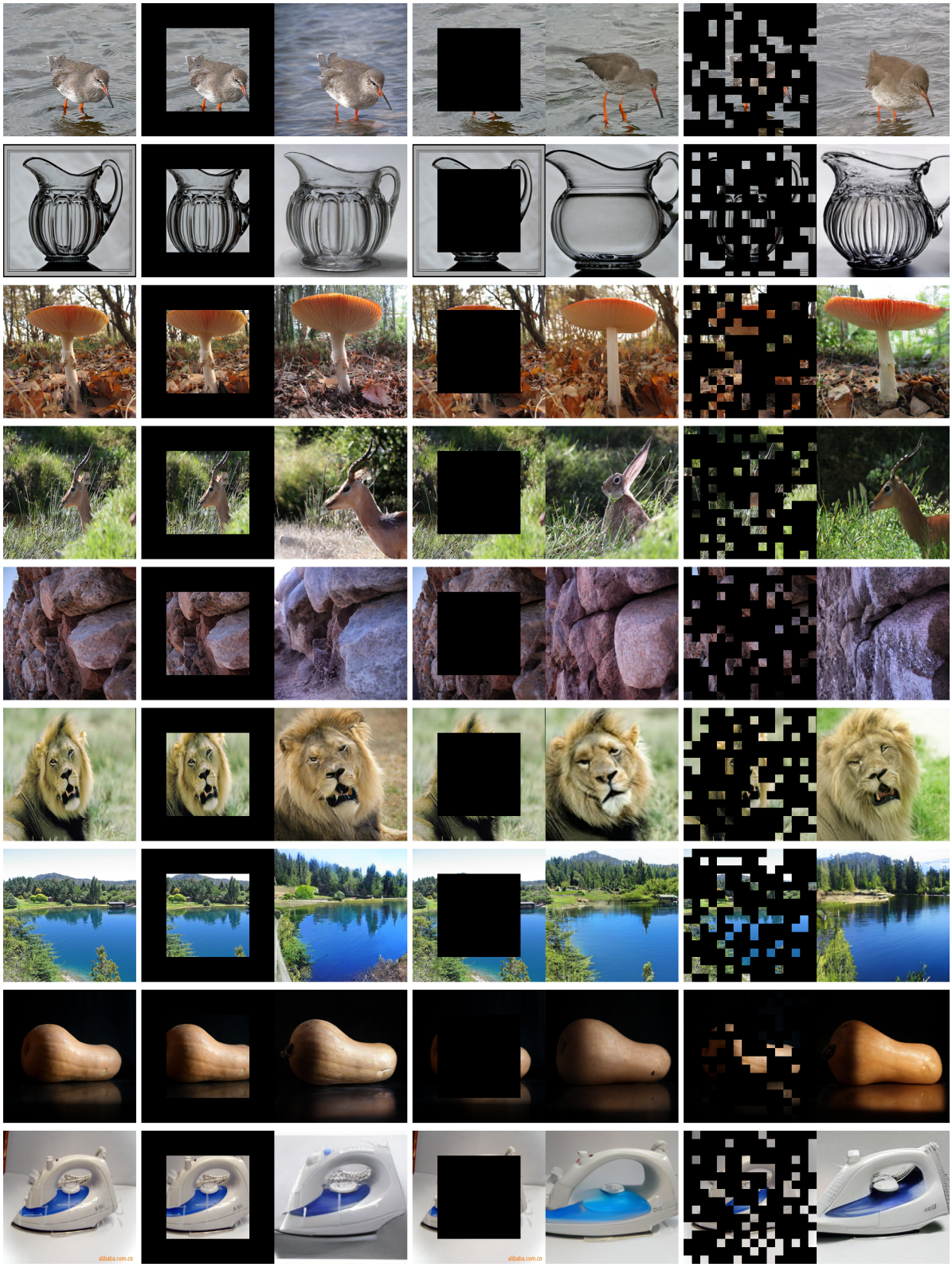


Figure 12. Examples of image inpainting, outpainting and reconstruction with Sorcen ViT-B. The first column is the original image.

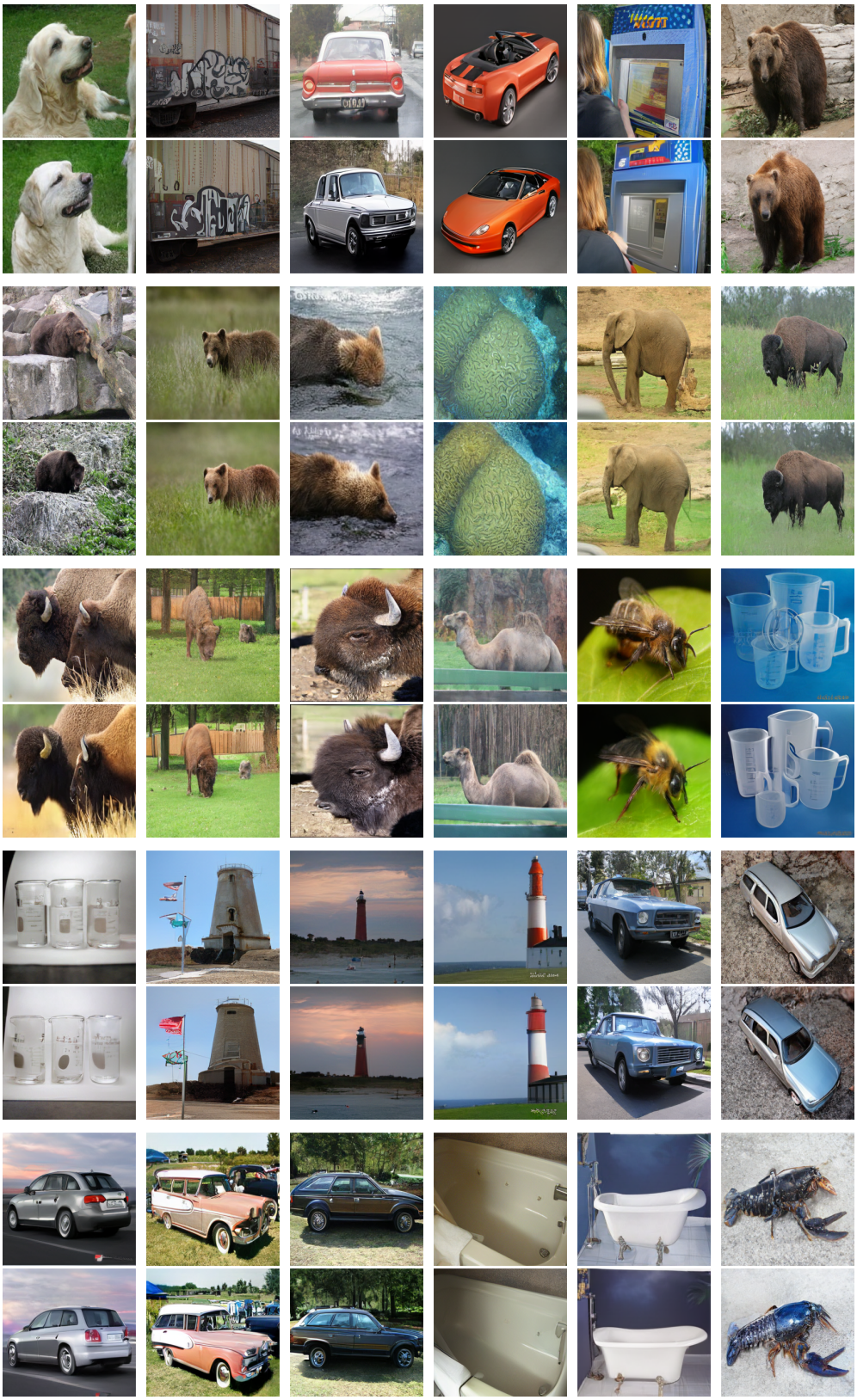


Figure 13. Uncurated collection of Echo samples generated during Sorcen training for contrasting. For each couple of rows, the top one contains the original image, and the bottom one the Echo.



Figure 14. Uncurated collection of Echo samples generated during Sorcen training for contrasting. For each couple of rows, the top one contains the original image, and the bottom one the Echo.